

# Fuel cell/battery passive hybrid powertrain with active power sharing capability

Bernard J.<sup>1</sup>, Hofer M.<sup>1</sup>, Hannesen U.<sup>2</sup>, Toth A.<sup>3</sup>, Tsukada A.<sup>1</sup>, Büchi F.N.<sup>1</sup>, Dietrich P.<sup>1</sup>

<sup>1</sup> Paul Scherrer Institut, CH-5232 Villigen-PSI, Switzerland.

<sup>2</sup> Belenos Clean Power Holding, Faubourg du Lac 6, CH-2502 Bienne, Switzerland.

<sup>3</sup> Swatch Group, Faubourg du Lac 6, CH-2501 Bienne, Switzerland.

Corresponding author: [jerome.bernard@psi.ch](mailto:jerome.bernard@psi.ch)

**Abstract**—In a passive hybrid topology, the fuel cell is directly electrically coupled to the battery. Although no DC/DC converters are used, it is possible to control the fuel cell power by adjusting its operating pressure, and thus the power sharing between the fuel cell and the battery becomes actively controlled. Using this concept, simulations results show that the power demand of an electric vehicle is fulfilled while sustaining the battery state of charge. By removing the DC/DC converter, the hybrid system becomes simpler, lighter and cheaper.

## I. INTRODUCTION

In a fuel cell hybrid vehicle, the primary power source is based on a polymer electrolyte fuel cell system (PEFC) [1-4] which converts hydrogen and oxygen into electrical power with only water and heat as byproducts. The battery is used as an energy buffer [5,6]; it power assists the fuel cell system during peak power demands (vehicle acceleration), it recovers partially the kinetic energy of the vehicle during braking phases, and it allows shifting to a certain degree the fuel cell operating point for optimizing the efficiency. The battery is usually used in a charge sustaining mode, i.e. the state of charge evolves around a prescribed value and no external charger is used.

In a passive hybrid architecture (Fig. 2), the fuel cell and the battery are directly connected to the bus without DC/DC converter(s). Therefore, contrary to an active hybrid architecture (Fig. 1), the two components operate at the same voltage [7], which brings several constraints and disadvantages [8-11]. Upon all the problems, the bus voltage and the currents regulate themselves according to the impedance of the fuel cell system and the battery, which means that the system variables (currents, voltage, powers, state of charge) are uncontrolled (no power management strategy is possible) and can therefore reach or exceed their limits, leading eventually to a system breakdown.

Although the active hybrid architecture (Fig. 1) has been established as the preferred topology, this paper shows that a passive hybrid can become a suitable solution for powertrain applications when the power sharing becomes

actively controlled. The active power sharing is achieved by controlling the operating pressure of the fuel cell, which varies its internal impedance. Since there are no DC/DC converters, the passive hybrid is the cheaper and the simpler solution, and the power losses in the electronic hardware are eliminated.

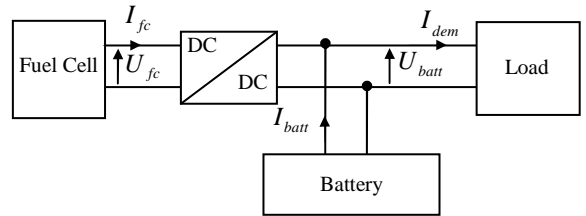


Fig. 1. Active fuel cell/battery hybrid topology.

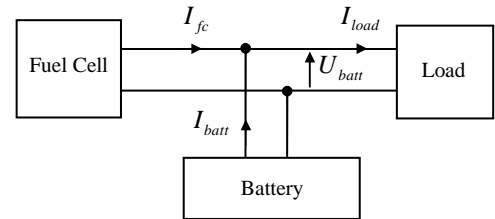


Fig. 2. Passive fuel cell/battery hybrid topology.

In the first part of this paper, the characteristics of the fuel cell system are presented. A pure  $H_2/O_2$  fuel cell system is considered in this approach, and it is shown how the fuel cell power is controlled. Then in the next section the simulation model of the passive hybrid powertrain is given. Section 4 provides simulation results. The last part of the paper discusses the advantages and the drawbacks of the passive hybrid solution.

## II. FUEL CELL SYSTEM

The fuel cell system considered is a  $H_2/O_2$  PEFC system. Such a system using pure oxygen as the oxidant is not commonly used for powertrain applications where the  $H_2$ /air fuel cell systems are dominating. A  $H_2/O_2$  PEFC system brings yet several advantages such as higher

specific power, higher efficiency, higher system dynamics and easier water management [12]. The main disadvantages are the need of oxygen production and its on board storage, but this can be balanced by the higher efficiencies achieved by such powertrains [13].

Fig. 3 shows a simplified scheme of a  $H_2/O_2$  PEFC system for automotive application [12-13]. It is composed from a PEFC stack surrounded by auxiliary components grouped into three main circuits (Fig. 3): 1) the hydrogen circuit on the anode side, 2) the oxygen circuit on the cathode side and 3) the cooling circuit. The cathode and anode pressures are controlled by means of proportional valves. The hydrogen and oxygen gases are re-circulated from stack outlet to stack inlet by means of recirculation pumps. The recirculation loops contain also water separators and purge valves which are not shown on Fig. 3.

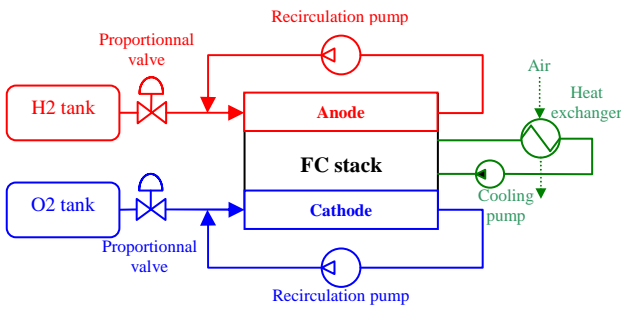


Fig. 3. Simplified scheme of a  $H_2/O_2$  fuel cell system.

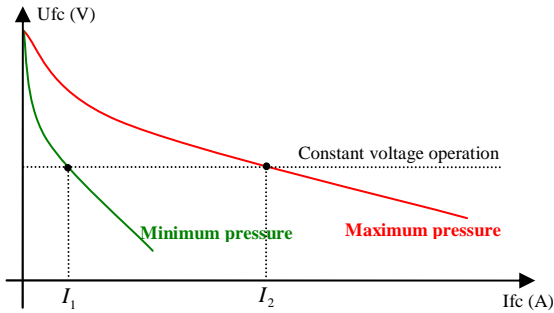


Fig. 4. Example of polarization curves of a fuel cell stack at different operating pressures.

The electrical characteristic of a fuel cell is described by its polarization curve (Fig. 4). This polarization curve is pressure and temperature dependent. For instance, at a constant temperature and a constant voltage, the fuel cell current decreases when decreasing the gas pressures (Fig. 4). This feature is interesting because it means that the current of a fuel cell system operating at constant voltage can be adjusted with the pressure: the minimum pressure gives the minimum current ( $I_1$ , Fig. 4) and the maximum pressure gives the maximum current ( $I_2$ , Fig. 4).

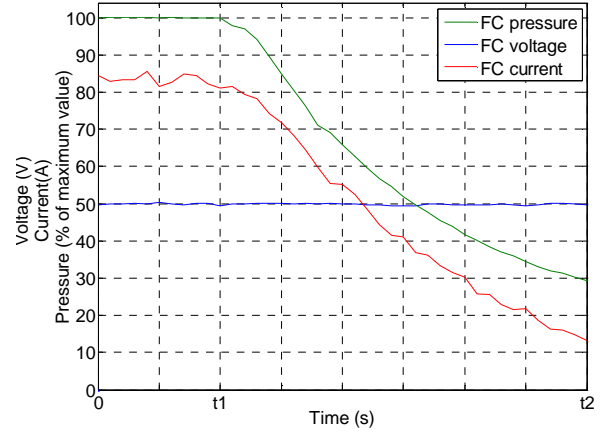


Fig. 5. Current and pressure variation with an  $H_2/O_2$  PEFC system operating at constant voltage.

Fig. 5 shows experimental results performed with a 10kW fuel cell stack operated in a laboratory testbench. The load connected to the FC stack operated at a constant voltage of 50V. Until  $t=t_1$ , the FC pressure (cathode and anode pressures) is nominal and the corresponding current is 85A. Then between  $t=t_1$  and  $t=t_2$ , the FC pressure is reduced from 100% to 30% of nominal value, which concomitantly decreases the FC current from 85A to near 13A. Considering the results from Fig. 4 and Fig. 5, it means that in the case of a passive hybrid where the battery operates at a nearly constant voltage, the fuel cell current power can be actively controlled.

### III. PASSIVE HYBRID POWERTRAIN SIMULATION

#### A. Fuel cell model

In a first approach, a steady state model of the fuel cell system is considered [1]. The model uses real experimental data to simulate a full scale fuel cell stack. The polarization curves have been measured at nominal temperature for different operating pressures. The parasitic load for the  $H_2/O_2$  system (consumption of auxiliary components) is estimated at constant 2% of the nominal power.

A pressure variation rate is also considered in the model. In a  $H_2/O_2$  fuel cell system, the pressures at the anode and cathode can increase quickly (positive rate higher than 0.5 bar/s). This fast positive rate is constrained by the dynamic of the proportional valves and by their orifices sections (defining the maximum gas flow). Pressure reductions are achieved by closing the proportional valves (Fig. 3) while drawing a fuel cell current. Assuming that the anode and the cathode have similar volumes, the negative rate is constrained by the oxygen consumption only. This negative rate can be estimated according to the FC current and the cathode parameters (when water vapor is neglected):

$$\dot{p}_{O_2}(t) = \frac{\dot{n}_{O_2}(t) \cdot R \cdot T_{fc}(t)}{V_{cathode}} \quad (1)$$

$$\text{with } \dot{n}_{O_2}(t) = \frac{I_{fc}(t)}{4 \cdot F} \cdot N_{cell} \quad (2)$$

with  $\dot{p}_{O_2}$  the pressure decrease rate (Pa/s),  $R$  the ideal gas constant ( $\text{m}^2 \text{kg s}^{-2} \text{K}^{-1} \text{mol}^{-1}$ ),  $\dot{n}_{O_2}$  the oxygen consumption rate (mol/s),  $T_{fc}$  the fuel cell mean temperature (K),  $V_{cathode}$  the total volume of the cathode gas circuit ( $\text{m}^3$ ),  $I_{fc}$  the stack current (A),  $N_{cell}$  the number of cells in the stack and  $F$  the faraday number (C).

As example, with a volume of 5 liters of the cathode gas circuit, a 200 cell stack operating at  $80^\circ\text{C}$  and a current of 150 A, a pressure decrease rate of 0.45 bar/s is achieved. The achievable increasing and decreasing pressure rates allow for sufficient dynamics of the fuel cell power for the automotive powertrain application.

### B. Battery model

The equivalent circuit model retained for the battery is composed from a voltage source in series with a resistor [14,15]. The open circuit voltage and the internal resistor are function of the state of charge:

$$C_{batt}(t) = C_{batt}(0) - \int_0^t \eta_f(SOC(u), \text{sign}(I_{batt}(u))) \cdot I_{batt}(u) \cdot du \quad (3)$$

$$SOC(t) = \frac{C_{batt}(t)}{\overline{C_{batt}}} \quad (4)$$

with  $C_{batt}$  the battery capacity,  $\overline{C_{batt}}$  the nominal capacity,  $\eta_f$  the faradic efficiency and  $I_{batt}$  the battery current.

The battery voltage  $U_{batt}$  depends on the state of charge  $SOC$  and on the current  $I_{batt}$ :

$$U_{batt}(SOC, I_{batt}) = OCV_{batt}(SOC) - R_{batt}(SOC, \text{sign}(I_{batt})) \cdot I_{batt} \quad (5)$$

with

$$R_{batt}(SOC, \text{sign}(I_{batt})) = \begin{cases} R_{charge}(SOC) & \text{if } I_{batt} \leq 0 \quad (\text{charge}) \\ R_{discharge}(SOC) & \text{if } I_{batt} > 0 \quad (\text{discharge}) \end{cases} \quad (6)$$

The battery cell parameters are given in Table 1.

TABLE 1  
BATTERY CELL PARAMETERS

Cell type	Li-Ion	Faradic efficiency	99 %
Nominal voltage	3.6V/cell	Peak current	350 A
Nominal capacity	33Ah	Maximum voltage	4.1 V/cell
Internal resistance	1 mΩ/cell	Minimum voltage	2 V/cell

### C. Powertrain model

(1)  
The passive hybrid power source composed by the battery and the fuel cell supply the electric powertrain of a light passenger car. The power demand is calculated with an energetic model of a car driving a defined speed cycle. This power demand is adjusted by the auxiliary power to take into account the consumption of the fuel cell auxiliaries. The parameters of the vehicle are provided in Table 2.

TABLE 2  
VEHICLE PARAMETERS

Vehicle mass	1000kg	Motor peak power	120kW
Aero.drag coeff.	0.35	Motor avg. efficiency	80 %
Frontal area	1.9 m <sup>2</sup>	Motor peak efficiency	95 %
Rolling resistance	0.009	DC/AC efficiency	95 %
Motor continuous power	60 kW	DC/AC cst. power	300W

### D. Power management strategy

The power sharing between the fuel cell and the battery needs to be defined. It is chosen to regulate the bus voltage around a prescribed setpoint. Ideally, this setpoint corresponds to the nominal battery voltage, which ensures that the state of charge stays around its nominal value. A controller adjusts the fuel cell operating pressure according to the bus voltage variation. The control loop is resumed in Fig. 6.

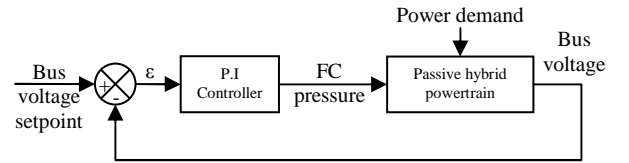


Fig. 6. Fuel cell pressure controller in passive hybrid powertrain.

## IV. SIMULATION RESULTS AND DISCUSSION

A simulation result is given Fig. 7 for the US06 driving cycle. It shows that the power demand of the powertrain is satisfied by the fuel cell passive hybrid power source. The fuel cell pressure controls the bus voltage around a prescribed voltage, which makes the battery state of charge evolving near 50%. The bus voltage remains within the fuel cell voltage range and the battery voltage range specified. Similar results were achieved with other driving (urban, outer-urban, highway) and the passive hybrid architecture was able to fulfill the power demand of the motor.

These encouraging results were achieved by considering a pure H<sub>2</sub>/O<sub>2</sub> fuel cell system. This kind of FC system is an advantage in the proposed passive hybrid architecture because it is possible 1) to vary quickly the system pressure and 2) to follow fast current transitions without having fuel or oxidant starvations phenomena. These properties allow fulfilling the power demand of aggressive driving cycles. More careful considerations and

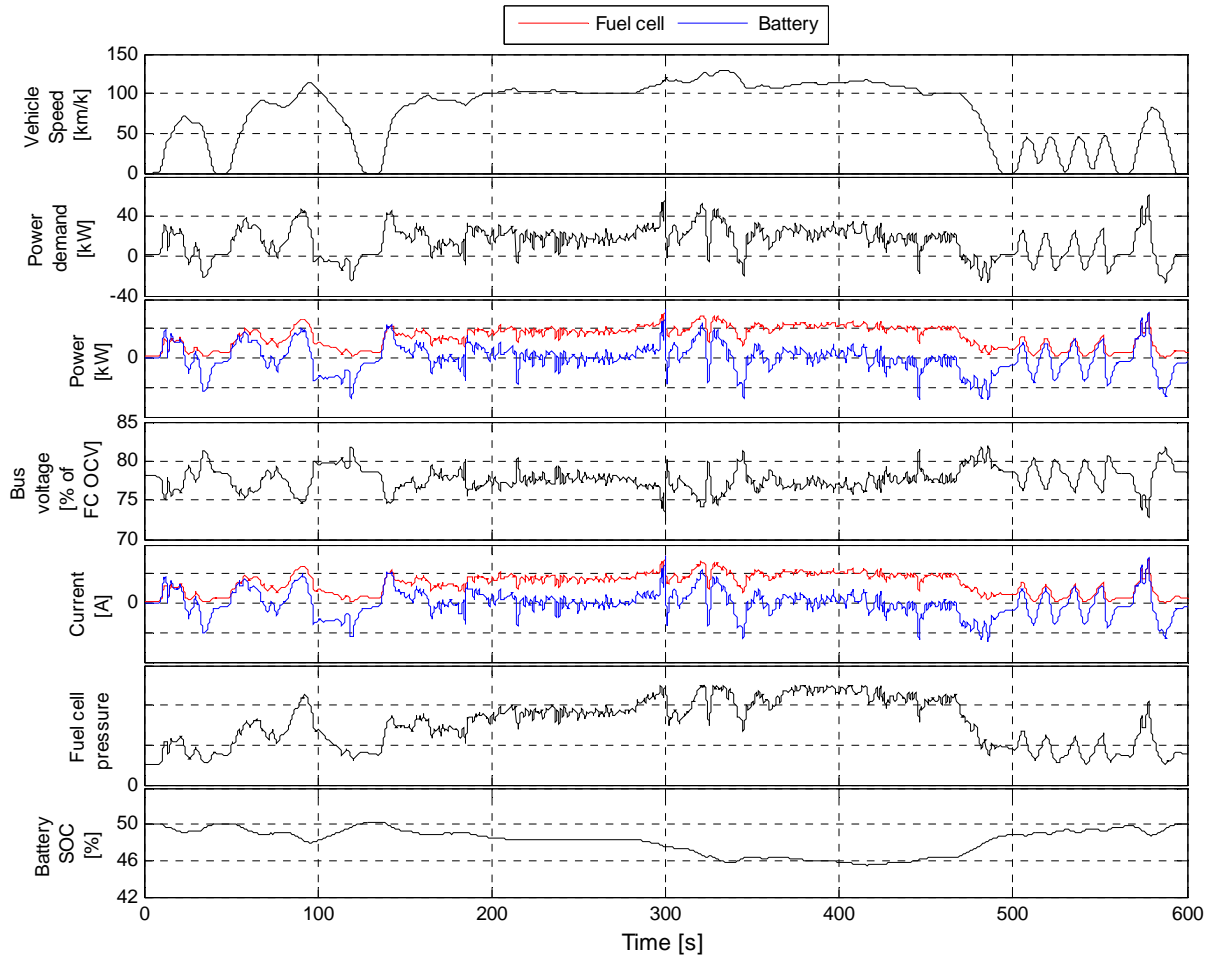


Fig. 7: Simulation of the passive hybrid powertrain for the US06 driving cycle.

investigations would be needed to consider an H<sub>2</sub>/air fuel cell system.

In this concept of passive hybrid, it is also important to note that the fuel cell system is forced to operate at pressures lower than its nominal value, which reduces its efficiency. This is however balanced by the absence of DC/DC converter losses. Current investigations revealed that the fuel consumption of a fuel cell passive hybrid powertrain is on average similar than those achieved with an active hybrid topology. The global efficiency is even higher when driving on high speed and/or aggressive driving cycles because the high power and high energy demands forces the fuel cell to operate at its nominal pressure, so its nominal efficiency, without losses in a DC/DC converter.

At last, since the fuel cell and the battery voltages are equal, the sizing of each device needs to be considered carefully. The degree of freedom in sizing is considerably reduced as compared to the active hybrid architecture [16] where the DC/DC converter(s) adapts voltages to the bus

voltage. The battery voltage operating range is defined by its maximum voltage in charge and its minimum voltage in discharge (Fig. 8). This range must fit into the fuel cell voltage operating range to avoid permanent degradation of one or the other device.

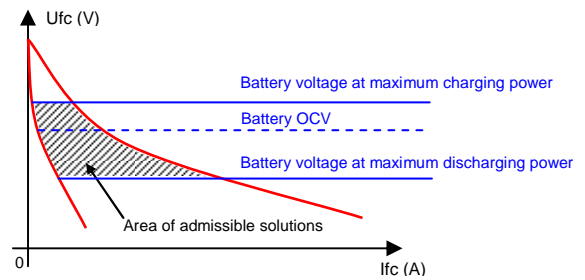


Fig. 8: Operating range (shaded area) limited by the fuel cell (red) and the battery (blue) limits in the passive hybrid topology.

## V. CONCLUSION

The paper shows that a fuel cell passive hybrid power source is a practicable solution for powertrain application when the power sharing becomes actively controlled. Here the fuel cell power is adjusted by controlling the fuel cell pressure. Eliminating the DC/DC converters makes the system easier, lighter, smaller, and the power losses in the hardware are reduced. However, it is important to define the correct battery and fuel cell parameters in order that both devices operate in a matched voltage range.

Current works are devoted to experimental validations. A fuel cell and a battery of practical size for automotive application are currently under development. Laboratory experiments should provide additional evidences about the feasibility of the concept.

## ACKNOWLEDGMENT

The present research work has been supported by the Belenos Clean Power Holding. The authors gratefully acknowledge the support.

## REFERENCES

- [1] D.D. Boettner, G. Paganelli, Y.G. Guezennec, G. Rizzoni, M.J. Moran, *Proton Exchange Membrane (PEM) fuel cell system for automotive vehicle simulation and control*, Journal of Energy Resources Technology, vol. 124, pp. 20-27, 2002.
- [2] P. Dietrich, F.N. Büchi, A. Tsukada, M. Bärtschi, R. Kötz, G.G. Scherer, P. Rodatz, O. Garcia, M. Ruge, M. Wollenberg, P. Lück, A. Wiartalla, C. Schönfelder, A. Schneuwly, P. Barrade, *HyPower-a technology platform combining a fuel cell system and a supercapacitor*, Handbook of fuel cells-fundamentals, technology and applications, vol. 4, pp. 1184-1198, 2003.
- [3] A. Emadi, K. Rajashekara, S. Williamson, S. Lukic, *Topological Overview of Hybrid Electric and Fuel Cell Vehicular Power System Architectures and Configurations*, IEEE Transaction on Vehicular Technology, Vol. 54, 2005.
- [4] P. Dietrich, D. Laurent, G. Paganelli, A. Tsukada, D. Walser, P.A. Magne, F.N. Büchi, P. Varenne, R. Kötz, S. Freunberger, *Concept, Design and First Results of the Light-Weight-Fuel-Cell-Vehicle «HY-LIGHT»*, EVS 21, Monaco, 2005.
- [5] T. Markel, M. Zolot, K.B. Wipke, A.A. Pesaram, *Energy storage requirements for hybrid fuel cell vehicles*, Advanced Automotive Battery Conference, Nice, 2003.
- [6] K.S. Jeong, B.S. Oh, *Fuel economy and life-cost analysis of a fuel cell hybrid vehicle*, Journal of Power Source, Vol. 105, pp. 58-65, 2002.
- [7] M.J. Blackwelder, R.A. Dougal, *Power coordination in a fuel cell-battery hybrid power source using commercial power controller circuits*, Journal of Power Sources, vol. 134, pp. 139-147, 2004.
- [8] R. Saisset, C. Turpin, S. Astier, J.M. Blaquièrre, *Electricity generation starting from a fuel cell hybridized with a storage device*, Vehicle Power and Propulsion Conference, Paris, 2004.
- [9] Z. Jiang, L. Gao, M. Blackwelder, R.A. Dougal, *Design and experimental tests of control strategies for active hybrid fuel cell/battery power sources*, Journal of Power Sources, Vol. 71, pp. 130-163, 2004.
- [10] L. Gao, Z. Jiang, R.A. Dougal, *Evaluation of Active Hybrid Fuel Cell/Battery Power Sources*, IEEE Transactions on Aerospace and Electronic Systems, vol. 41, pp. 346-355, 2005.
- [11] Z. Jiang, R.A. Dougal, *A Compact Digitally Controlled Fuel Cell/Battery Hybrid Power Source*, IEEE Transaction on Industrial Electronics, vol. 53, 2006.
- [12] F.N. Büchi, S.A. Freunberger, M. Reum, G. Paganelli, A. Tsukada, P. Dietrich, A. Delfino, *On the Efficiency of an Advanced Automotive Fuel Cell System*, Fuel Cells, vol. 7, pp. 159-164, 2007.
- [13] F.N. Büchi, G. Paganelli, P. Dietrich, D. Laurent, A. Tsukada, P. Varenne, A. Delfino, R. Kötz, S.A. Freunberger, P.A. Magne, D. Walser, D. Olsommer, *Consumption and Efficiency of a Passenger Car with a Hydrogen/Oxygen PEFC based Hybrid Electric Drivetrain*, Vol. 7, pp. 329-335, 2007.
- [14] V.H. Johnson, *Battery performance models in ADVISOR*, Journal of Power Sources, vol. 110, pages 321-329, 2002.
- [15] J. Van Mierlo, P. Van den Bossche, G. Maggetto, *Models of energy sources for EV and HEV: fuel cells, batteries, ultracapacitors, flywheels and engine-generators*, Journal of Power Sources, Vol. 128, pp. 76-89, 2004.
- [16] J. Bernard, S. Delprat, F.N. Büchi, T.M. Guerra, *Fuel-Cell Hybrid Powertrain: Toward Minimization of Hydrogen Consumption*, IEEE Transactions on Vehicular Technology, vol. 58, pp. 3168-3176, 2009.